*Macromolecules* **1993,** *26,* 4420–4425

# Water Induced Crystalline Transition of Polyamide 6,6: A Combined X-ray and Molecular Modeling Approach

**C. Vergelati,[†] A. Imberty,[‡] and S. Pérez[*,§]**

*Rhône Poulenc Recherches, Centre de Recherches des Carrières, 85 Avenue des Frères Perret, BP 62, 69192 Saint-Fons Cédex, France, Laboratoire de Synthèse Organique, Faculté des Sciences et Techniques, 2 Rue de la Houssinière, 44072 Nantes Cédex 03, France, and Institut National de la Recherche Agronomique, Rue de la Géraudière, BP 527, 44026 Nantes Cédex 03, France*

*Received August 4, 1992; Revised Manuscript Received May 19, 1993*

ABSTRACT: Combined X-ray and molecular modeling approaches have been used to characterize and rationalize the crystalline transition displayed by polyamide 6,6 upon temperature and water treatment. Polyamide 6,6 material as processed by extrusion exhibits crystalline features close to those reported for the pseudohexagonal $\alpha_2$ phase. Upon storage, the water uptake induces solid state polymorphic transitions. This results in an evolution of the crystalline moiety toward the so-called $\alpha_1$ triclinic form. This phenomenon is reversible under temperature treatment. Modeling of the preferred three-dimensional organizations of polyamide 6,6 chains shows that several of these structures are energetically stable. They correspond to intermediate arrangements between the $\alpha_1$ and $\alpha_2$ phases. Further modeling of water interaction with an assembly of polyamide 6,6 chains indicates that water does not penetrate the crystalline part. Instead, by reacting with the crystalline surfaces, more preferentially with the *bc* plane, it induces the structural evolution from $\alpha_2$ to $\alpha_1$. Suggestions about the interactions between water molecules and the amorphous phases are also presented.

## Introduction

The temperature and the sorption of water have dramatic effects on the structural and mechanical properties of polyamide 6,6. The usual consequences of thermal treatment such as annealing yield an increase in crystallinity of the polymeric material.[1] Subsequent significant reductions in impact strength and elongation to break are observed. As for water uptake, the change from dryness to saturation at room temperature is responsible for a 4-fold decrease in the modulus of unoriented polymer.[2] The effect of water on some properties of oriented polyamide 6,6 have been interpreted in terms of crystalline domains having their largest dimension in the hydrogen bond direction.[3] From the sorption and the desorption isotherms of water on amorphous polyamide 6,6, it has been suggested[4] that three water molecules are sorbed on two neighboring amide groups in the accessible regions of the material (see Figure 1 for a schematic representation of the polymer).

Crystalline polyamide 6,6 is precipitated from solution, either from methanol or from glycerol or ethylene glycol,[5] and well oriented samples can be obtained. Fiber X-ray crystallography has helped identify the crystalline arrangement taken by the polymer chains in this so-called $\alpha_1$ phase[6] having a triclinic unit cell. Under temperature treatment, the phenomenon is clearly reversible: a change from the triclinic cell to a pseudohexagonal form, the $\alpha_2$ phase, is observed; it is referred to as the Brill transition.[7,8] No confusion should be made between the $\alpha_2$ pseudohexagonal form and the so-called $\alpha_{II}$ phase which results from crystallization by quenching.[1] In the pseudohexagonal form, the *c* axes and the polymer chains are still tilted with respect to the *ab* plane, but the projection of the unit cell onto a plane normal to the *c* axis is metrically hexagonal. The variations of the unit cell as a function of temperature have been reported.[5,9] However, a detailed description of this three-dimensional structure is not available. Table I summarizes the crystal data for the $\alpha_1$ and $\alpha_2$ phases, whereas the projections of the two structures are shown in Figure 2.

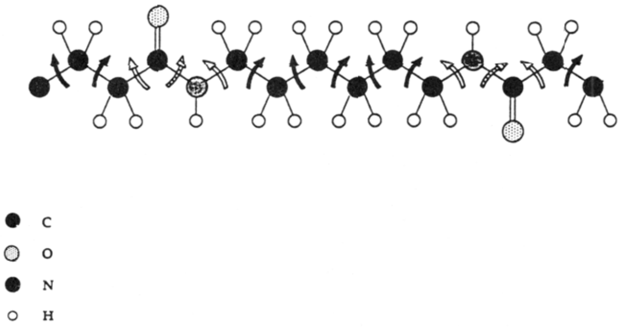

**Figure 1.** Schematic drawing of the repeating unit of polyamide 6,6, along with the atomic types.

The elucidation of the molecular basis responsible for some physical properties and/or polymorphic transitions still remains a major objective. Many recent advances in the theory and application of molecular modeling to structural elucidations of polymers have produced a wide range of useful results. It is the goal of the present work to provide a molecular vision of the reversible polymorphic transition occurring in the solid state, as well as to elucidate the role of water molecules in promoting such an evolution.

## Materials and Methods

**Experimental Procedures.** Extruded polyamide 6,6 samples were characterized by wide angle X-ray scattering (WAXS) using Cu K$\alpha$ radiation. Digital data were collected in a fixed time mode at intervals of 0.02° in $2\theta$. The $2\theta$ scale was calibrated with polypropylene as an internal standard. Moisture treatment was accomplished by exposing the samples to room conditions at 22 °C and 60% relative humidity for 30 days. The evolution of the crystalline structure was followed by X-ray diffractometry every 15 days. For the sake of comparison, one X-ray diffractogram

---

[*] To whom correspondence should be addressed. Tel: (33)-40.67.50.43. Fax: (33)40.67.50.05.

[†] Centre de Recherches des Carrières.

[‡] Laboratoire de Synthèse Organique.

[§] Institut National de la Recherche Agronomique.

0024-9297/93/2226-4420$04.00/0 © 1993 American Chemical Society

**Table I. Crystal Data for $\alpha_1$ and $\alpha_2$ Phases of Polyamide 6,6**

| crystal data | $\alpha_1$ phase[a] | $\alpha_1$ phase[b] (24 °C) | $\alpha_2$ phase[b] (202 °C) |
|---|---|---|---|
| $a$ (Å) | 4.9 | 4.95 | 4.92 |
| $b$ (Å) | 5.4 | 5.44 | 6.04 |
| $c$ (Å) | 17.2 | 17.38 | 17.23 |
| $\alpha$ (deg) | 48.5 | 48.3 | 53.5 |
| $\beta$ (deg) | 77.0 | 76.6 | 80.7 |
| $\gamma$ (deg) | 63.5 | 62.6 | 60.5 |
| $V$ (Å$^3$) | 302.5 | 308.0 | 351.0 |
| $d_{calc}$ | 1.240 | 1.219 | 1.069 |
| $\Delta\theta$ (deg)[c] | 120 | 104 | 0 |

[a] Bunn and Gardner.[6] [b] Starkweather and Jones.[5] [c] $\Delta\theta = \theta(010) - \theta(100)$.

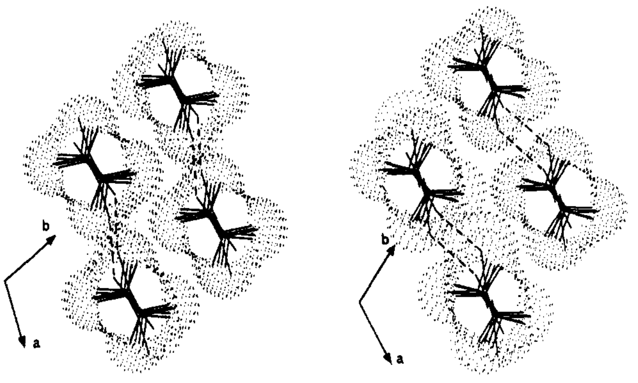

a) b)

**Figure 2.** Projection on the $ab$ plane of the crystalline arrangement of (a) the $\alpha_1$ phase from the work of Bunn and Gardner[6] and (b) the $\alpha_2$ phase, constructed from the unit cell parameters proposed by Starkweather and Jones,[5] at 202 °C. van der Waals surfaces truncated at 5 Å along the fiber repeat axis are displayed as dots, whereas the hydrogen bonds are shown as dashed lines.

was recorded on a polyamide 6,6 sample submitted to accelerated aging, i.e. 2 h at 150 °C under the antogeneous pressure of water.

The part of the X-ray diffractogram ranging from 0 to 35 ° in $2\theta$ was refined with the decomposition method described by Tran and Buléon.[10] The position of each individual reflection was calculated, the peak shape being fitted with a Pearson VII type function. The refinement of the $d$ spacings corresponding to the crystalline phases were performed using an optimization method based on a COMPLEX type procedure.[11] Due to the low amount of experimental data, parameters were refined in two steps: first $b$, $\alpha$, and $\gamma$ were refined while $a$, $c$, and $\beta$, the parameters which define the hydrogen bonded sheet, were given their equilibrium values; second, $a$, $c$, and $\beta$ were refined while the other data were kept fixed in their optimized values. Finally, the contribution arising from the amorphous component was subtracted from the experimental spectrum.

**Computational Procedures.** The starting geometry of one repeating unit of polyamide 6,6 in its all *trans* conformation was taken from the crystal structure of the $\alpha_1$ phase.[6] The hydrogen atoms were generated in theoretical positions, the C–H and N–H bonds being given the magnitude derived from neutron diffraction data. The complete repeating unit (Figure 1) was then submitted to a thorough refinement through molecular mechanics calculations.

The modeling of polymer–polymer interactions was conducted by following a procedure reported recently.[12–14] This method is quite appropriate for predicting the packing relationship of two polymer chains and for studying polymorphism. Given a rigid model of an isolated polymer chain, its interaction with a second chain is studied at varied helix-axis translations and mutual rotational orientations while the helices are kept in van der Waals contact. In the chain pair modeling, it is assumed that the two chains, A and B, are regular helices. Their periods must be commensuarate, and the chains can only be parallel or antiparallel to one another. A set of four interhelical parameters is required in order to define the geometric orientation of chain A relative to chain B. These are $\mu_A$ and $\mu_B$, rotations of the chains A and B about their axes from 0 to 360°; $\Delta_x$ and $\Delta_z$ represent positional shifts normal and parallel to the identity axes, respectively.

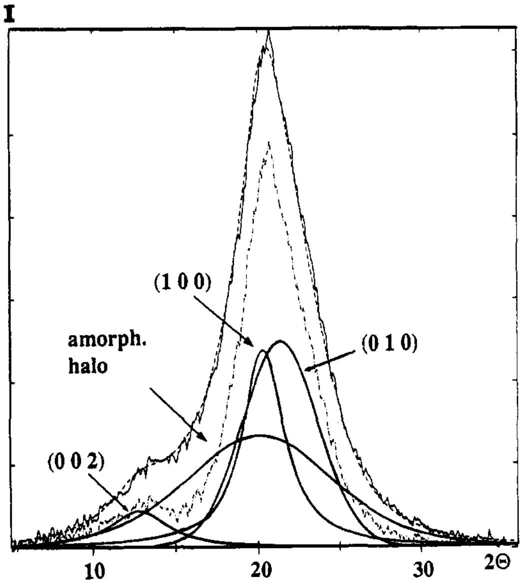

**Figure 3.** Wide angle X-ray scattering pattern of a polyamide 6,6 sample processed by extrusion: experimental (full line) and calculated diagram (dashed line), including individual peaks (with appropriate indexing) and amorphous halo. The dashed-dotted line corresponds to the subtraction of the amorphous component from the experimental diagram.

The interaction energy of the two chains is considered to be the sum over all pairwise atom–atom interactions. Such interactions are calculated according to 6–12 potential functions.[15] As for the energy stabilization arising from hydrogen bonding, an extra term has to be included. In this case, a simple energy criterion is used, based on the distance between oxygen and nitrogen atoms which can interact through hydrogen bonding.[16] For these purposes, a computer program was developed which could be interfaced with the CHEM-X software package.[17]

Water–polyamide 6,6 interactions were simulated using molecular mechanics methods with the CHEM-X force field.[17] Point charges on atoms of the polymer repeat unit were derived from semiempirical calculations with the use of the MNDO Hamiltonian.[18] They were kept unchanged over the duration of the simulation. The hydrogen bonds were taken into account by following the expression given by McGuire *et al.*[19] and using the magnitude derived by Garcia and Starkweather.[20] The minimization was performed on a set of three water molecules interacting with four polymer chains. The polymer chains were constrained to remain in a crystallographic register. They were allowed for rotational and translational motions along the fiber axis (from 0 to 360° and 0 to half a fiber repeat, respectively). Only small translational motions along the crystallographic axes $a$ (4.5 Å < $a$ < 6.0 Å) and $b$ (5.0 Å < $b$ < 6.5 Å) were investigated. The motions of the water molecules were unconstrained.

## Results and Discussion

**X-ray Diffraction.** The wide angle X-ray scattering pattern recorded on a polyamide 6,6 sample processed by extrusion is shown in Figure 3. This is a typical experimental diagram which can be decomposed as indicated in the Materials and Methods section. Appropriate removal of the contribution arising from the amorphous halo reveals the presence of three diffraction peaks which can be indexed as (010), (100), and (002), by analogy with the triclinic unit cell.[6] Quite interestingly, this X-ray diffractogram does not correspond to the $\alpha_2$ type of structure. The changes of the three-dimensional polymer structure upon aging and subsequent water uptake are depicted in Figure 4. The three diffractograms have been recorded at 15-day intervals. The striking feature is the variation of the $d$ spacings of reflections (100) and (010) which indicate a significant evolution of the crystal lattice. After 30 days, the water uptake reaches equilibrium around

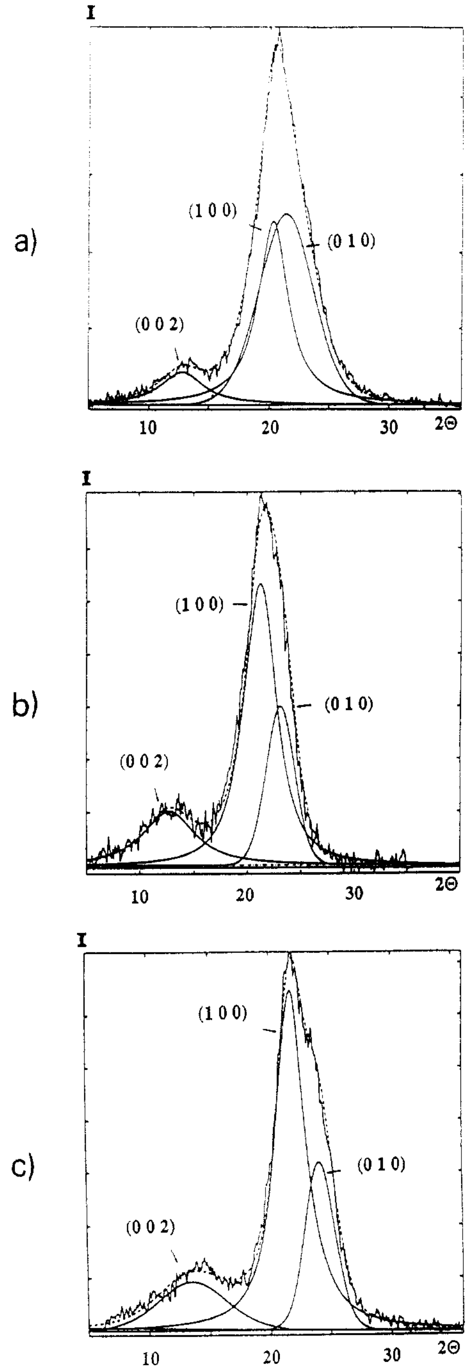

**Figure 4.** Reconstructed wide angle X-ray scattering pattern of a polyamide 6,6 sample after amorphous halo removal, as a function of aging: (a) just after extrusion; (b) after 15 days of storage at room temperature and 60% relative humidity; (c) after 30 days of storage at room temperature and 60% relative humidity.

2.25% (w/w) and no further changes of the crystalline unit cell are detected for this type of storage. This observation is also reflected by the asymptotic value reached by $\Delta\theta$ ($\theta(010) - \theta(100)$) which indicates a variation of the structural arrangement toward the $\alpha_I$ phase. Nevertheless, such a phase, for which a typical wide angle X-ray scattering diagram is shown in Figure 5, is never reached under the conditions used for the storage of the polymer. Table II summarizes these structural changes in terms of variations of unit cell dimensions. Quite interestingly, we observed that aging is accompanied by an increase of the fiber repeat dimension. This finding is in agreement with recent molecular dynamics calculations[21] which indicate that some segmental molecular motions are likely to occur along the *c* fiber direction.

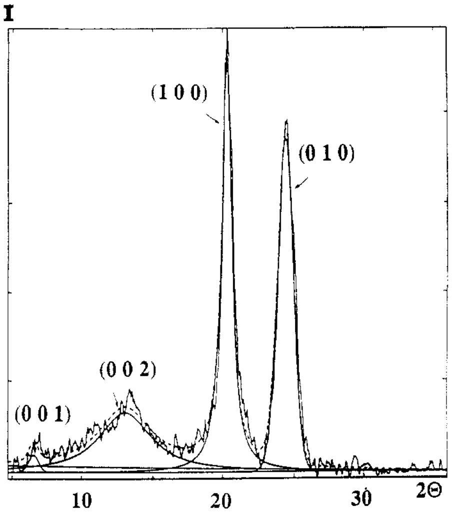

**Figure 5.** Reconstructed wide angle X-ray scattering pattern of a polyamide 6,6 sample submitted to accelerated aging during 2 h at 150 °C under vapor pressure in an autoclave. The amorphous halo has been removed.

**Table II. Evolution of the Unit Cell Dimensions of Polyamide 6,6 as a Function of Time Storage at Room Temperature and 60% RH and Comparison with the Sample Submitted to Accelerated Aging**

| | sample | | | |
|---|---|---|---|---|
| cryst data | as such | 15 days | 30 days | accelerated |
| $a$ (Å) | 5.15 | 4.99 | 5.03 | 5.00 |
| $b$ (Å) | 5.96 | 5.55 | 5.82 | 5.28 |
| $c$ (Å) | 17.44 | 17.40 | 17.53 | 17.75 |
| $\alpha$ (deg) | 53.0 | 54.3 | 50.2 | 49.8 |
| $\beta$ (deg) | 76.5 | 78.8 | 79.5 | 75.1 |
| $\gamma$ (deg) | 58.6 | 58.4 | 57.0 | 61.4 |
| $V$ (Å$^3$) | 362.4 | 328.9 | 319.5 | 313.3 |
| $d_{calc}$ | 1.035 | 1.140 | 1.174 | 1.197 |
| $\Delta\theta$ (deg)[a] | 28 | 47 | 58 | 110 |
| water uptake (w/w) | 0.00 | 2.22 | 2.25 | 17.00 |

[a] $\Delta\theta = \theta(010) - \theta(100)$.

**Chain–Chain Interactions.** The *a priori* modeling of the chain association was intended to provide understanding of how crystal structures form as well as describing all the low energy chain pairing which may occur in the noncrystalline regions. In the present investigation, the starting information was the *trans* conformation of the polyamide 6,6 chains. In a first step, all the possible arrangements occurring between two polyamide 6,6 chains were examined (Figure 6). This was performed by rotating $\mu_A$ and $\mu_B$ over the whole angular range from 0 to 360° by increments of 10 deg. The relative displacement ($\Delta_z$) of the chains was investigated over the whole length of the fiber repeat by 0.5-Å increments. For each setting of the chains, as a function of $\mu_A$, $\mu_B$, and $\Delta_z$, the magnitude of the perpendicular off-set $\Delta_x$ was computed according to the contact procedure. The value of the energy corresponding to each set of chain orientations as defined by the set of four interhelical parameters, was evaluated. Within the three-dimensional space ($\mu_A$, $\mu_B$, and $\Delta_z$), the search for the energy minima was performed. The results indicated that the significant energy minima occurred for values of $\mu_A$ and $\mu_B$ such that $\mu_A = \mu_B$. The coupling of $\mu_A$ and $\mu_B$ rotation angles suggests that the relative packing of neighboring chains of polyamide 6,6 is best achieved through translational symmetry. From now on, the investigation was conducted by assuming that $\mu_A = \mu_B$. This allows for a straightforward two-dimensional study, and the variations of $\Delta_x$ have been calculated as a function of the translation $\Delta_z$ along the fiber axis and the coupled rotation angle $\mu_A = \mu_B$.

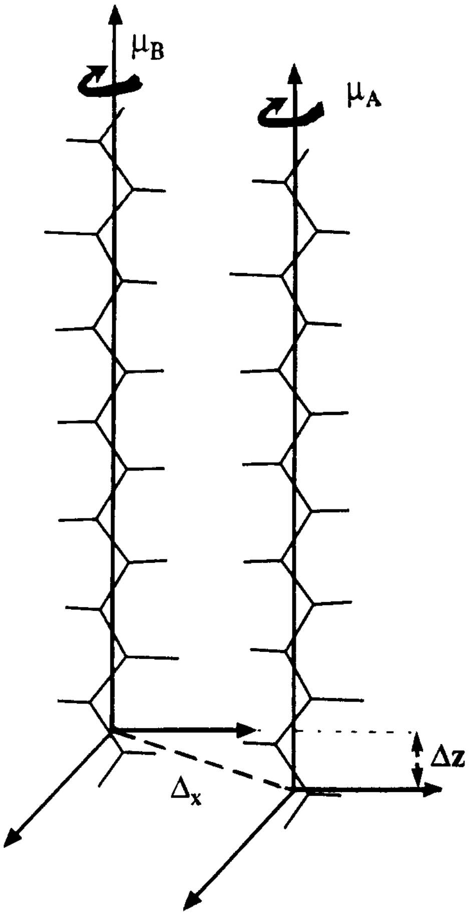

**Figure 6.** Interhelical parameters required to define the geometric orientation of chain A and chain B of polyamide 6,6.

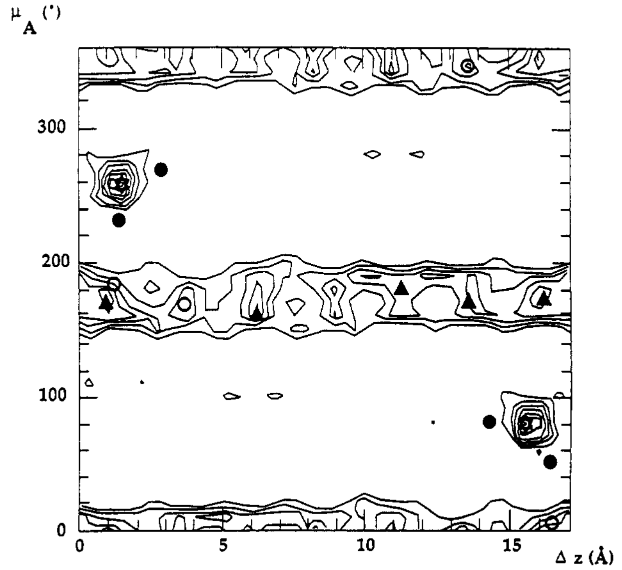

**Figure 7.** Interchain energy contour maps as a function of the translation $\Delta_z$ along the fiber axis of polyamide 6,6 and the coupled rotation $\mu_A = \mu_B$, corresponding to perpendicular off-set $\Delta_x$ satisfying the contacting procedure *between two single chains of polyamide 6,6*. Contours have been drawn at intervals of 5 kcal/mol. * indicate low energy arrangements in which the polyamide chains are associated by hydrogen bonds; ▲ indicate low energy arrangements in which the polyamide chains pack only through van der Waals interactions (as along the *b* axis in Figure 2); ● indicate the orientation between two chains as observed in $\alpha_1$ and $\alpha_2$ phases (as along the *a* axis in Figure 2); ○ indicate the orientation between two chains as observed in $\alpha_1$ and $\alpha_2$ phases (as along the *b* axis in Figure 2).

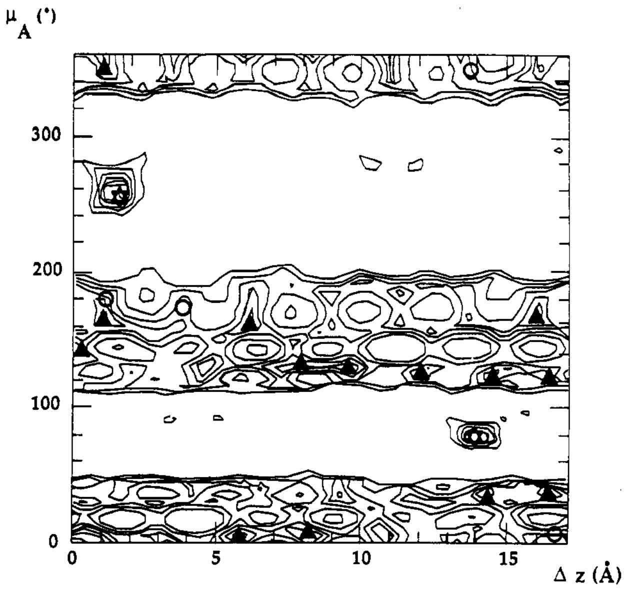

**Figure 8.** Interchain energy contour maps as a function of the translation $\Delta_z$ along the fiber axis of polyamide 6,6 and the coupled rotation $\mu_A = \mu_B$, corresponding to perpendicular off-set $\Delta_x$ satisfying the contacting procedure *between one single chain and a pair of polyamide 6,6 chains having the orientation $\mu_A$ = 80° and $\Delta_z$ = 15.2 Å*. Contours have been drawn at intervals of 5 kcal/mol. * indicate low energy arrangements in which the polyamide chains are associated by hydrogen bonds; ▲ indicate low energy arrangements in which the polyamide chains pack only through van der Waals interactions (as along the *b* axis in Figure 2); ○ indicate the orientation between one single chain and a pair of polyamide 6,6 chains as observed in $\alpha_1$ and $\alpha_2$ phases (as along the *b* axis in Figure 2).

Figure 7 is a representation of the variations of the interchain energy corresponding to the optimum perpendicular off-set, $\Delta_x$, as a function of translations, $\Delta_z$, along the chain direction and coupled rotations of $\mu_A$ and $\mu_B$. For the first duplex, the optimum value of $\Delta_x$ is 4.7 Å. The map exhibits an obvious symmetry which is due to the centers of symmetry within the repeat unit of the polymer chain. Consequently, only one section needs to be described. Low energy domains are found which correspond to a somewhat restricted range of $\mu_A$ values and an extended range of $\Delta_z$ values. Within these domains, several energy minima are found, the locations of which are reported in Figure 7 along with those corresponding to the chain pairing observed in the $\alpha_1$ and $\alpha_2$ phases. The lowest energy interchain pairing corresponds to an arrangement where intermolecular hydrogen bonding of the type N–H···O occurs. However, it does not correspond to the organizations observed in the two polymorphs which display this type of hydrogen bonding. In contrast, one of the secondary low energy minima corresponds closely to the situation observed for another type of chain pairing in the two crystalline polymorphs. The occurrence of several energy minima in the vicinity of $\mu_A$ = 180° for values of $\Delta_z$ ranging from 0 to 17.2 Å indicates that there are many stable ways to pair parallel chains of polyamide 6,6. All these pairings correspond to chain–chain interactions where all the contacts are of the van der Waals type. Obviously, such situtations may occur in the amorphous phase of the polymer.

The second step of the investigation was concerned with the setting of all the possible arrangements occurring between a pair of polyamide 6,6 chains having the orientation corresponding to the lowest energy and a single chain. Figure 8 is a representation of the variation of the interchain energy corresponding to the optimum perpendicular off-set, $\Delta_x$, as a function of translations, $\Delta_z$, along the chain direction and rotations of $\mu_A$. The calculated map in Figure 8 no longer displays any symmetry. The

**Table III. Lattice Constants Predicted from Theoretical Packing Calculations**

| cryst data | lattice 1 | lattice 2 | lattice 3 | lattice 4 | lattice 5 |
|---|---|---|---|---|---|
| $a$ (Å) | 4.91 | 4.91 | 4.91 | 4.91 | 4.91 |
| $b$ (Å) | 5.37 | 5.62 | 5.68 | 5.31 | 5.62 |
| $c$ (Å) | 17.2 | 17.2 | 17.2 | 17.2 | 17.2 |
| $\alpha$ (deg) | 50.2 | 47.7 | 48.1 | 49.7 | 47.7 |
| $\beta$ (deg) | 69.5 | 69.5 | 69.5 | 69.5 | 69.5 |
| $\gamma$ (deg) | 84.3 | 83.4 | 83.5 | 80.5 | 65.5 |
| V (Å$^3$) | 321.4 | 328.8 | 329.3 | 319.1 | 317.6 |
| $\Delta\theta$ (deg)[a] | 66 | 62 | 51 | 79 | 62 |

[a] $\Delta\theta = \theta(010) - \theta(100)$.

section of the map corresponding to values of $\mu_A$ ranging from 160 to 340° is identical to the same section of the map shown in Figure 7. Several alterations are observed in the remaining part of the map such as the occurrence of new energy minima. Among them, five subsequent stable three-dimensional organizations of chains in a latticelike fashion can be obtained. Predicted crystal parameters derived from these lattice models are described in Table III. These data correspond to unit cells of polyamide 6,6 which would be intermediate between the two reported $\alpha_1$ and $\alpha_2$ phases. In this way, theoretical packing calculations seem to correlate well with experimental data.

**Water Induced Polymorphic Transformation.** As presented above, there are many circumstances whereby a transition from the pseudohexagonal $\alpha_2$ phase to the triclinic $\alpha_1$ phase can be observed in which hydration is the driving force. For the modeling study, the starting system was made up of four chains of polyamide 6,6 having the orientations found in the $\alpha_2$ phase, plus water molecules. The starting locations of these water molecules was derived from a previous analysis.[4] One of the water molecules is firmly bound to two adjacent carbonyl groups from two different chains; the other water molecules are in proximity of the N–H bond of the chain, located half a period away from the previous arrangement. The water molecules are interacting with the $bc$ plane of the cell. The energy minimization was performed with the geometric constraints described in the Materials and Methods section. After 200 cycles of energy refinement an intermediate hydrated organization is reached. There are still two polyamide 6,6 chains which interact through N–H···O hydrogen bonds in a way which differs from the starting arrangement of the $\alpha_2$ phase. As for the chains interacting directly with water molecules, they have switched toward a stable arrangement which prefigures the $bc$ plane found in the $\alpha_1$ phase. The lack of translational symmetry between the polymer chains of the intermediate phase indicates that such an arrangement cannot extend over a long distance and cannot be considered as a nuclei for crystal growth. Nevertheless, the intermediate organization remains stable when submitted to further energy refinement. By alteration of the boundary conditions on the $a$ and $b$ axes (i.e. 4.5 Å $< a <$ 5.3 Å and 5.8 Å $< b <$ 6.2 Å) another stable arrangement is found after about 100 cycles of energy minimization. Within this refinement, the major changes occur between the polymer chains which are directly hydrogen bonded. Only minor changes are observed for the locations of the water molecules. The overall arrangement of the polyamide 6,6 chains corresponds very closely to the $\alpha_1$ phase. It has to be noted that, within the set of boundary conditions used in the present simulation, there is no evidence whatsoever for the water molecules to dissociate the interchain arrangements and penetrate further the "crystalline" domains.

The computer simulation would not be thorough without investigating the situation where the water molecules are interacting with the $ac$ plane of the cell. Even with the set of periodic conditions mentioned above, is has never been possible, in our hand, to reach any convergence.

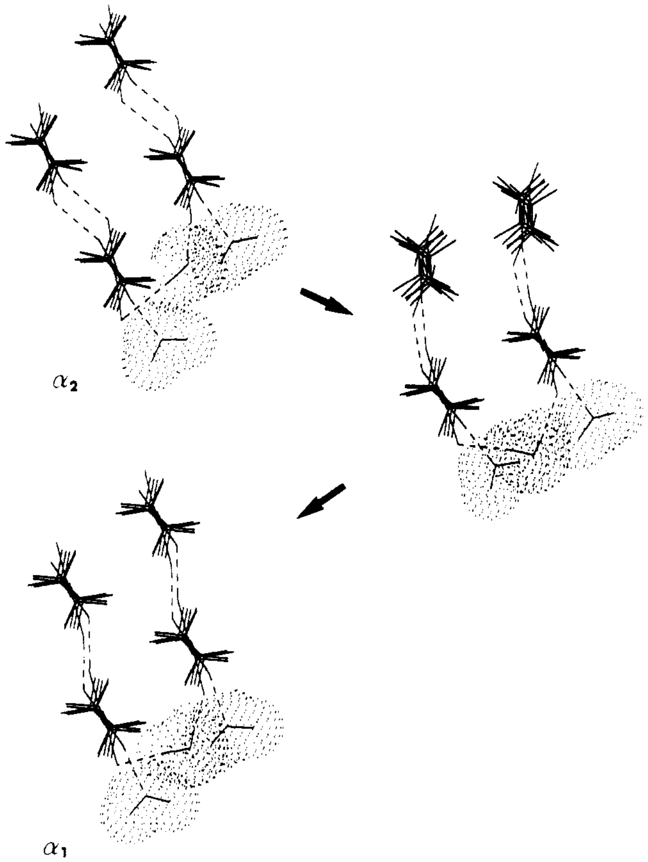

**Figure 9.** Model of the polymorphic transition from the $\alpha_2$ phase to the $\alpha_1$ phase for polyamide 6,6 in the solid state. The van der Waals surfaces of the water molecules are shown with dots; the hydrogen bonds are shown as dashed lines.

The present work helps in understanding the polymorphic transitions occurring in polyamide 6,6 and provides insights into intimate molecular details associated with such a transition. For the first time, a transition pathway from the $\alpha_2$ to the $\alpha_1$ crystalline phases is suggested which incorporates the participating role of water molecules. There is also the occurrence of a stable intermediate stage which may very well explain the slowness of the reverse Brill transition. Water molecules induce a progressive rotation of the chains in a two step process. A schematic representation of such a polymorphic pathway is depicted in Figure 9. Such a scheme may not operate on a long distance range and cannot involve cooperative motion of an entire crystal. Indeed, Starkweather[22] concluded from excess heat capacity measurements that the Brill transition occurs point by point involving small groups of adjacent polyamide chains. This is in contrast with what has been suggested in the case of polyamide 6 where the polymorphic transition is caused by the swelling by water of the noncrystalline regions.[23]

In agreement with the results[24,25] derived from solid state $^2$H NMR we conclude that water molecules have to be excluded from the crystalline regions. Nevertheless, the $\alpha_2$–$\alpha_1$ transition requires some minute amount of water which presumably is located within the interlamellar amorphous phase. The size of the crystals in polyamide 6,6 has been estimated[22] to be on the order of 100 Å. One may deduce that in a typical sample obtained from crystallization in water, and exhibiting 50% crystallinity and a global water uptake of 9% (w/w), only 1% (w/w) of water would go to the interlamellar amorphous phase, the remaining 8% (w/w) being located in the intrinsic amorphous phase. Therefore, there is, on average, one water molecule per two carboxylamide groups (or one water per repeat unit of polyamide 6,6). In the amorphous phase, the amount of carboxylamide groups involved in hydrogen bonding of the N—H···O=C type, is on the order of 95%. One may conclude that the great majority of water molecules located in the amorphous phase tend to associate to ultimately form clusters when the equilibrium state is reached.[26,27]

## Conclusions

The present work has demonstrated that after being processed by extrusion, polyamide 6,6 displays an X-ray diffraction pattern close to, albeit nonidentical, the pseudohexagonal $\alpha_2$ phase. Upon storage at room temperature and relative humidity of 60% the polymer undergoes a slow polymorphic transition toward the triclinic $\alpha_1$ form, without reaching it. Both $\alpha_1$ and $\alpha_2$ phases seem to correspond to extreme cases, respectively induced by water and temperature. Our modeling study provides detailed molecular comprehension of how such an $\alpha_2$–$\alpha_1$ transition may be induced by water; the existence of stable structural intermediates is obviously required in such a solid state transition. Within the range defined by the $\alpha_2$ and $\alpha_1$ forms other stable three-dimensional arrangements are also viable, as indicated by the experimental data and the modeling of chain–chain interactions. The present results also suggest that only a fraction of the water uptaken by the polymer may be actively implied in promoting the transition. This results in an accumulation of water molecules in the amorphous region. Because of the high cohesive forces present between polyamide chains in the amorphous part, the water molecules are forced to aggregate in a cluster type fashion.

**Acknowledgment.** The authors thank Mr. Gauthier-Lafaye and Mr. Jarry (Rhône Poulenc S.A.) who gave their agreement for the publication of this work.

## References and Notes

(1) Starkweather, H. W., Jr.; Whitney, J. F.; Johnson, D. R. *J. Polym. Sci., Part A* **1963**, *1*, 715.
(2) Starkweather, H. W., Jr. In *Nylon Plastics*; Kohan, M. I., Ed.; Wiley: New York, 1973; Chapter 9.
(3) Starkweather, H. W., Jr. *J. Macromol. Sci., Phys.* **1969**, *B3*, 727.
(4) Puffr, R.; Sebenda, J. *J. Polym. Sci., Part C* **1967**, *16*, 79.
(5) Starkweather, H. W., Jr.; Jones, G. A. *J. Polym. Sci., Polym. Phys. Ed.* **1981**, *19*, 467.
(6) Bunn, C. W.; Gardner, E. V. *Proc. R. Soc. London, Ser. A* **1947**, *189*, 39.
(7) Brill, R. *J. Prakt. Chem.* **1942**, *161*, 49.
(8) Brill, R. *Makromol. Chem.* **1956**, *18/19*, 294.
(9) Starkweather, H. W., Jr.; Zoller, P.; Jones, G. A. *J. Polym. Sci., Polym. Phys. Ed.* **1984**, *22*, 1615.
(10) Tran, V. H.; Buléon, A. *J. Appl. Crystallogr.* **1987**, *20*, 430.
(11) Nelder, J. A.; Mead, R. *Comput. J.* **1965**, *7*, 308.
(12) Scaringe, R. P.; Pérez, S. *J. Phys. Chem.* **1987**, *91*, 2394.
(13) Pérez, S.; Imberty, A.; Scaringe, R. P. In *Computer Modeling of Carbohydrate Molecules*; French, A. D., Brady, J. W., Eds.; ACS Symposium Series 430; American Chemical Society: Washington, DC, 1990; pp 281–299.
(14) Pérez, S. In *Electron Crystallography of Organic Molecules*; Fryer, J. R., Dorset, D., Eds.; NATO ASI Series 328; Kluwer Academic Publishers: Dordrecht, The Netherlands, 1991; pp 33–53.
(15) Scott, R. A.; Scheraga, H. A. *J. Chem. Phys.* **1966**, *45*, 2091.
(16) Pérez, S.; Vergelati, C. *Polym. Bull.* **1987**, *17*, 141.
(17) *CHEM-X, Molecular Modeling Software*; Chemical Design Ltd.: Oxford, England.
(18) Dewar, M. J. S.; Thiel, W. *J. Am. Chem. Soc.* **1977**, *99*, 4899.
(19) McGuire, R. P.; Momany, F. A.; Scheraga, H. A. *J. Phys. Chem.* **1972**, *76*, 375.
(20) Garcia, D.; Starkweather, H. W., Jr. *J. Polym. Sci., Polym. Phys. Ed.* **1985**, *23*, 537.
(21) Wendoloski, J. J.; Gardner, K. H.; Hirschinger, J.; Muira, H.; English, A. D. *Science* **1990**, *247*, 431.
(22) Starkweather, H. W., Jr. *Macromolecules* **1989**, *22*, 2000.
(23) Murthy, N. S.; Stamm, M.; Sibilia, J. P.; Krimm, S. *Macromolecules* **1989**, *22*, 1261.
(24) Hirschinger, J.; Miura, H.; Gardner, K. H.; English, A. D. *Macromolecules* **1990**, *23*, 2153.
(25) Miura, H.; Hirschinger, J.; English, A. D. *Macromolecules* **1990**, *23*, 2169.
(26) Hernandez, R. J. Ph.D. Dissertation Thesis, Michigan State University, 1989.
(27) Vergelati, C. Unpublished results.